CCCARD2014-49

CORROSION WALL LOSS AND OXIDE FILM THICKNESS ON SCWR FUEL CLADDING

M. Edwards[1], S. Rousseau[1], D. Guzonas[1]
[1] Atomic Energy of Canada Limited, Chalk River, Ontario, Canada

Abstract

The three key materials performance metrics of the Canadian Supercritical Water-cooled Reactor (SCWR) core internals, and particularly those of the fuel cladding, are the lifetime wall loss due to corrosion, the oxide thickness developed on the cladding between fuel cycles, and the likelihood of cracking. Other materials performance requirements are mitigated by design. The present paper establishes acceptance criteria for corrosion wall loss and oxide film thickness of the fuel cladding and evaluates the corrosion performance of Alloy 800, Alloy 214, and Alloy 625 with respect to these criteria.

1. Introduction

The Canadian SCWR pressure-tube reactor concept benefits from several design features that mitigate the challenges of materials selection for core internals. In-core materials are required to meet the often-conflicting demands for neutron economy, high-temperature strength, ductility, corrosion resistance and resistance to irradiation damage. To meet these demands, the Canadian SCWR concept employs zirconium-alloy pressure tubes that operate below 100 ºC, providing the strength needed for a pressure boundary while providing excellent neutron economy. A zirconia insulator is used to separate the pressure tube from the 625 ºC light water coolant. To ensure the insulator maintains performance, it forms part of the fuel assembly and is replaced every 3.5 years. The fuel assembly is supported structurally by a central rod within the flow tube, where it is surrounded by the subcooled inlet coolant at 350 ºC. The only parts of the fuel assembly exposed to supercritical water and irradiation are the flow tube, liner tube and the fuel cladding. Of these, the fuel cladding experiences the highest temperature and thus its performance is of greatest concern.

Several classes of alloys can be immediately excluded from discussion as fuel cladding for the SCWR. It has been known since the early 1970s that traditional zirconium alloy cladding experiences high corrosion rates in supercritical water (SCW) [1]. Although some Zr-Fe-Cr alloys showed promise at 500 ºC [2], the work of Khatamian [3] showed that these alloys can also experience breakaway corrosion at that temperature. Chromium coating of zirconium alloys was shown to significantly reduce corrosion and hydrogen uptake [3], but the reliability of a coating must always be carefully considered. Likewise, ferritic steels are known to experience significant corrosion at temperatures relevant to the SCWR [4]. Ferritic steels also have an α/β transition temperature of 912 ºC [5], which could be surpassed under accident conditions. Ferritic-martensitic steels experience comparable weight gains to zirconium alloys [6], and can be excluded. Others

have explored Ti-base alloys, and found them to have similar oxide weight gains to ferritic-martensitic steels [7]. The consensus in the Generation IV SCWR community has been to narrow the scope of interest to austenitic stainless steels and Ni-base alloys. Canada has selected five alloys, namely 347 SS, 310 SS, Alloy 800H, Alloy 625 and Alloy 214, as its prime fuel cladding alloy candidate.

The high-level acceptability criterion of the fuel cladding is that it cannot fail. Failure could occur by: through-wall corrosion, oxide build-up than can impede heat transfer, stress corrosion cracking (SCC), and stress exceeding the yield limits of the material (especially if the material is embrittled by irradiation). This paper addresses the first two in this list, but a brief discussion on the other topics is included for completeness.

1.1 Stress Corrosion Cracking

Ru and Staehle [8] discussed historical and contemporary work that has helped in our practical understanding of SCC. The pioneering work of Coriou et al. [9] showed that transgranular SCC (TGSCC) was experienced by austenitic alloys with less than 20 wt% Ni when exposed to Cl^-, while intergranular SCC (IGSCC) was experienced by alloys with greater than 60 wt% Ni when exposed to pure water. The work of Yonezawa and Onimura [10] has shown that increasing Cr content increases the time-to-cracking. Through the work of several researchers, Ru and Staehle [11] show that residual strains caused by cold-work and welds stimulate SCC and enhance crack growth rates.

Ru and Staehle [5][8][11] also discussed impurities such as Cl^- and Pb that are known to promote SCC. Chloride was a particular problem during the nuclear superheat program in the 1960s, and essentially forced the use of alloys with higher Ni content [5]. However, water purification techniques have improved in the decades since then, such that the feedwaters of current reactors and fossil-fired SCW plants typically contain less than 3 ppb Cl^- and 0.1 ppb Pb [11]. Additionally, SCW is denser than steam, and the solubility of impurities increases with increasing steam density. Direct precipitation of impurities in the SCWR is therefore less of a concern than in the nuclear superheat program. However, co-precipitation of impurities with corrosion products could provide a mechanism for concentrating impurities near the surface. Adding to this concern the possibility of water chemistry excursions and the expected presence of oxidizing radiolysis products in-core favours the selection of alloys with 20 – 60 wt% Ni.

Was et al. [12] provided a recent review of the SCC behaviour of several alloys in SCW. While a significant amount of data now exists on SCC in SCW, the data are often contradictory, often because of differences in test methodology. Little data exists on the effects of irradiation on SCC in SCW. Proton-irradiated 304 and 316L that was subsequently exposed to 400 ºC and 500 ºC SCW showed increased propensity for cracking compared to unirradiated samples [12][13]. Because the nature of the environment and the test method are so important to observations of SCC, it is important to conduct tests under relevant conditions. Most of the testing to date has been carried out at strain rates much higher than the expected in-service conditions.

1.2 Embrittlement

Stresses that exceed the yield limit on embrittled fuel cladding can also cause failure. Embrittlement is one manifestation of a decrease in fracture toughness (the ability to absorb impact) and is often measured as a decrease in elongation to fracture. Embrittlement can occur because the material is hardened, but can also occur as a result of a lack of cohesion at grain boundaries caused by precipitates or helium bubbles. An important design feature of the Canadian SCWR fuel cladding is that it is collapsible [14]. With the proper selection of fuel-cladding gap and cladding thickness, the cladding will collapse elastically onto the fuel pellet under the compressive stress of the coolant. Because the cladding is then supported by the fuel, the hoop stress becomes negligible and therefore the possibility of stress-induced failure is minimized. Nonetheless, to ensure that the collapse is elastic and to prevent longitudinal ridging, recent calculations have shown that a minimum cladding thickness of 0.4 mm is needed [14]. Other stresses must still be considered, such as hoop stresses caused by loss of coolant pressure and sudden expansion of fuel caused by a power surge, but a collapsible cladding affords minimal stress during normal operation and mitigates concerns about embrittlement.

High temperatures alone can cause embrittlement by increasing the kinetics of diffusion and precipitation [15]. Within the SCWR core, however, high temperatures are coupled with irradiation. The effects of radiation on grain boundary embrittlement are multiple: in a soft spectrum helium generated by the transmutation of ^{59}Ni to ^{56}Fe can diffuse to grain boundaries, radiation-generated defects can harden the matrix and also migrate to grain boundaries, with consequential enrichment or depletion of elements in response to that migration flux; typically Ni is enriched, while Cr is depleted at grain boundaries [16]. Grossbeck et al. [17] described the effects of irradiation on uniform elongation (a measure of ductility or lack thereof). Elongation data on 316 SS were gathered from several research reactors with differing He:dpa ratios, including fast reactors (where there is about 0.5 appm He:1 dpa), mixed-spectrum reactors (He:dpa ratio of about 75:1) and a tailored spectrum (He:dpa ratio of about 10:1). The results were presented as curves at 10, 20, 30 and 50 dpa. Lower He:dpa ratios resulted in less embrittlement, but at 10 dpa 316 SS showed uniform elongation below 0.5% in every reactor type at temperatures less than 400 °C [17]. Between 400 and 600 °C, uniform elongation was observed to increase up to ~5%, and then decrease at temperatures above 600 °C. These results are relevant to the Canadian SCWR where recent SPECTER analyses revealed that Alloy 800H fuel cladding would incur 9 dpa damage and generate 50 appm He after 3.5 years in-core—a He:dpa ratio of about 5:1.

It should be noted that cold-worked alloys retain more ductility after irradiation than solution-annealed alloys [18], although their unirradiated ductility is less due to work hardening. The cladding must possess some ductility (~2%) in order to deform initially. The amount of cold-work imparted on the cladding must be carefully considered to ensure sufficient initial ductility and post-irradiated ductility and strength. Cold-work also influences SCC behaviour and corrosion.

1.3 Corrosion Wall Loss Acceptance Criterion

It was mentioned above that the collapsible cladding must be a minimum thickness of 0.4 mm to prevent longitudinal ridging. However, it is also undesirable to have a cladding much thicker than 0.6 mm for reasons of neutron economy. Therefore, the maximum *corrosion allowance*, *a*, is:

$$a = 200\ \mu m \tag{1}$$

This number must provide for corrosion penetration, including average oxide penetration along grain boundaries, as well as fretting and other forms of wear for the in-core lifetime of the cladding, 30 600 h or 3.5 years [19].

1.4 Oxide Thickness Acceptance Criterion

Oxide build-up can occur both through deposition of corrosion products originating in the feedtrain and carried to the core by the coolant and through oxidation of the cladding. This oxide build-up can have a number of consequences. Oxide growth in tight geometries, such as between fuel pins, can exert force on members. The closest distance between fuel pins in the Canadian SCWR fuel assembly is 1240 µm, between pins of the inner ring. Although small, this is not a tight geometry from the perspective of oxide thickness.

The oxide may act as an insulator, leading to overheating and accelerated corrosion. With a constant heat flux, the exterior of the oxide at any given location has a constant temperature, regardless of thickness. Heat conduction through the oxide governs the cladding temperature. Very little is known about the nature of heat conduction through an oxide layer formed in SCW. In PWRs, pores in the oxide layer create a phenomenon known as wick boiling that enhances heat transfer through the oxide layer by adding a convective component [20]. It is not clear, however, if a similar mechanism would exist in an SCWR. At present, it may be conservative to assume a purely conductive mechanism of heat transfer. In light of this, the thicker the oxide, the hotter the fuel cladding; and the hotter the fuel cladding, the faster the rate of oxide growth.

Assuming a linear element rating (LER) around 40 kW/m and an oxide surface temperature around 800 ºC, the temperature increase across the oxide layer can be calculated by Eqn. (2), where q' is the LER, k_{eff} is the effective thermal conductivity of the oxide, r_i is the outside radius of the fuel pin and t_{oxide} is the thickness of the oxide. The effective thermal conductivity of a porous oxide layer was described by Cinosi et al. [20], given by Eqn. (3), where k_w is the thermal conductivity of water, k_{oxide} is the thermal conductivity of the solid oxide, ε is the porosity, and α is defined by Eqn. (4). A low effective thermal conductivity can be expected for a porous oxide layer in SCW, which has a lower thermal conductivity than the oxide itself. Supercritical water at 800 °C has a thermal conductivity of 0.12 $W \cdot m^{-1} \cdot K^{-1}$, while most oxides have a thermal conductivity in the range of 2 to 8 $W \cdot m^{-1} \cdot K^{-1}$ at the same temperature. Calculated results are shown in Figure 1; an oxide thermal conductivity of 3 $W \cdot m^{-1} \cdot K^{-1}$ was chosen as an approximate value within the range expected.

$$\Delta T = \frac{q'}{2\pi \cdot k_{eff}} \ln\left(\frac{r_i + t_{oxide}}{r_i}\right) \tag{2}$$

$$k_{eff} = k_w \left(\frac{1 - \left(1 - \alpha \frac{k_{oxide}}{k_w}\right)(1-\varepsilon)}{1 + (\alpha - 1)(1-\varepsilon)} \right) \tag{3}$$

$$\alpha = \left(\frac{3k_w}{2k_w + k_{oxide}} \right) \tag{4}$$

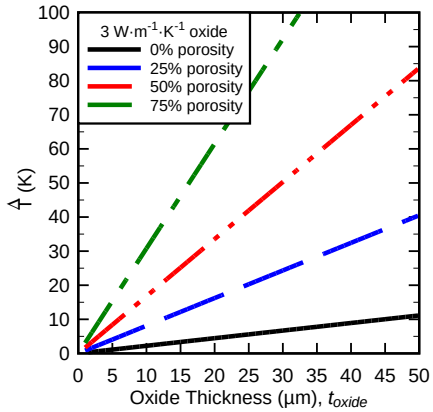

Figure 1: Temperature change across oxide layer as a function of oxide thickness and oxide porosity for an oxide with a thermal conductivity of 3 $W \cdot m^{-1} \cdot K^{-1}$ experiencing a 40 kW/m heat flux.

In the absence of a wick boiling analogue in the SCWR, the results of Figure 1 suggest that, for an initial cladding surface temperature of 800 ºC, the oxide must be compact and non-porous to avoid excessively high cladding temperatures. A major concern is oxide deposited from the coolant, as its porosity is likely to be high. In SCW fossil fired power plants, the weight of deposited oxide is about 4 times greater around the critical transition temperature than at higher temperatures [21]. Deposition model results suggest the weighting in the SCWR may be a more modest 1-2 times higher around the critical temperature transition [22]. Considering a fuel channel with coolant entering at 0.1 ppb Fe at a flow rate of 5 kg/s and having 9.5 m^2 of heated surface area, the *average* deposition, assuming complete precipitation, over a 10 200 h fuel cycle would be 0.5 µm of *non-porous* magnetite:

$$\frac{\left(0.1\times10^{-6}\,\text{g/kg Fe}\right)\left(5\,\text{kg/s}\right)\left(10200\,\text{h}\right)\left(3600\,\text{s/h}\right)}{\left(5.15\,\text{g Fe}_3\text{O}_4/\text{cm}^3\right)\left(\frac{167.4\,\text{g Fe}}{231.4\,\text{g Fe}_3\text{O}_4}\right)\left(9.5\,\text{m}^2\right)} \times \left(\frac{1\,\mu\text{m}}{\text{cm}^3/\text{m}^2}\right) \approx 0.5\,\mu\text{m} \tag{5}$$

It is reasonable to assume that the deposited oxide is porous; crud on present PWR fuel cladding is 80% porous [20]. Thus, the average thickness of deposited oxide may well be 2.5 µm. The immediate penalty, therefore, is approximately 10 K before any native oxide is considered.

The thickness of the native oxide is a function of growth rate at temperature and exfoliation rate. Sarver and Tanzosh [23] estimate the critical oxide thickness for exfoliation of austenitic stainless steels between 620 and 800 ºC as 15 µm. This value applies mostly to alloys that form a duplex oxide film where the differential thermal expansion between the layers cause stresses that lead to exfoliation. Tan et al. [24] showed that the oxide layers of Grain Boundary Engineered (GBE) Alloy 800H were less well defined, and provided evidence to suggest that it suffered less from exfoliation than the as-received sample. Some alloys, however, form a single layer of tightly-adherent chromium oxide, including many Ni-base alloys with high Cr contents. Through cold-work and shot-peening, many austenitic stainless steels can be made to form a thin chromium oxide layer by enhancing chromium diffusion through modified grain boundaries [23][25]. However, this benefit may disappear at high temperatures. Sarver and Tanzosh [23] have reported that the effects of shot-peening on corrosion of austenitic stainless steels in SCW disappeared somewhere between 620 and 750 ºC.

Exfoliation is undesirable, as it would contribute to activity transport and erode turbine blades. Therefore, the native oxide thickness of alloys that form a duplex oxide film should not exceed approximately 10 µm between fuel cycles, assuming a mechanical process will be applied to remove the outer layer of oxide scale between fuel cycles. Conservatively assuming that the native oxide is 50% porous, a 10 µm-thick oxide carries a temperature penalty of approximately 20 K (Figure 1). The total temperature gain across the oxide layer can therefore be taken to be 30 K. The calculated maximum (bare) cladding temperature for the Canadian SCWR is 800 ºC. The selected cladding material must therefore have an oxide thickness, t_{oxide} of:

$$t_{oxide} \leq 10\ \mu m \text{ at } 830\ ^{o}C \tag{6}$$

This number must provide for oxide growth over the time between fuel cycles, 10 200 h (425 d) [19]. Alloys forming a uniform and adherent oxide layer may be permitted a slightly thicker oxide, but the temperature difference across the oxide must be considered. (E.g., the corrosion of an alloy forming a 20 µm oxide must be evaluated at 800ºC + 10 K + 35 K = 845 ºC.) It must be remembered that increases in cladding temperature translate into increases in fuel centreline temperature.

2. Evaluation of Candidate Alloys against Acceptance Criteria

Three candidate alloys are considered below: Alloy 214, Alloy 800 and Alloy 625. These are evaluated with respect to the corrosion acceptance criteria established above. Scorecards for each alloy are presented at the end of each section (Tables 1-3).

2.1 Alloy 214

Alloy 214 contains 72 wt% Ni, which is undesirable for neutron economy, helium generation, irradiation damage and expected SCC resistance. Deodeshmukh et al. [26] reported that Alloy 214 is susceptible to strain-age cracking and hot cracking during welding [26]. Nonetheless, at only 16 wt% Cr, it is one of the most corrosion resistant alloys available [23]. Alloy 214 contains 4.4 wt% Al and owes its oxidation resistance to a tightly adherent alumina scale. Most alloys owe their corrosion resistance to a chromia scale, but chromia can oxidize and evaporate in SCW [27][28]. This will be especially true in SCW containing oxidizing radiolysis products. Alumina, on the other hand, cannot oxidize and is stable in high-temperature neutral water.

Reported corrosion testing of Alloy 214 in SCW is sparse. Sarver and Tanzosh [23] described corrosion tests of several alloys in steam at temperatures up to 800 ºC for advanced ultra-supercritical water boilers. They note that Alloy 214 showed the lowest corrosion rate of all alloys tested at 750 ºC and provided a parabolic (descaled) corrosion rate constant of ~2×10^{-16} $g^2cm^{-4}s^{-1}$. Based on this value, the expected metal loss after 3 fuel cycles (30 600 h) is 15 mg/dm^2 or about 0.2 µm penetration.

$$\begin{aligned}\Delta W &= (k_p t)^{0.5} \\ &= \left(\left(2\times10^{-16}\ \mathrm{g^2\cdot cm^{-4}\cdot s^{-1}}\right)\left(30600\ \mathrm{h}\right)\left(3600\ \mathrm{s/h}\right)\right)^{0.5}\left(1000\ \mathrm{mg/g}\right)\left(\frac{10\ \mathrm{cm}}{1\ \mathrm{dm}}\right)^2 \\ &= 15\ \mathrm{mg/dm^2}\end{aligned} \tag{7}$$

Deodeshmukh [29] reported the results of 360 day corrosion tests of foils of Alloy 214 and several nickel-base alloys in air with 10 vol% steam at 760 and 871 ºC. At 760 ºC, the metal loss was 0 µm, while at 871 ºC, the metal loss was 3 µm. The maximum internal oxide penetration measured by optical metallographic examination of eight locations was reported as 8 µm at 760 ºC and 23 µm at 871 ºC. The author reported an inner layer of Al_2O_3 and an outer layer of $NiAl_2O_4$ spinel, both less than 1 µm thick. While these results are not able to be directly translated to corrosion in SCW, they are encouraging.

Corrosion Penetration	0.2 µm at 750 ºC in steam (30 600 h) 8 µm at 760 ºC in air/10% steam (8640 h) 23 µm at 871 ºC in air/10% steam (8640 h)
Inner Oxide / Outer Oxide	Al_2O_3 / $NiAl_2O_4$
Native Oxide Thickness	< 2 µm at 871 ºC in air with 10% steam (8640 h)
Cracking Resistance	Susceptible to strain-age cracking Susceptible to hot cracking 72% Ni exceeds 60% limit

Table 1: Alloy 214 Scorecard

3. Alloy 800H

More is known about the corrosion behaviour of Alloy 800 and its variants in SCW than almost any other candidate alloy. Substantial research was conducted on Alloy 800 for the US nuclear superheat program in the 1960s. With 21% Cr and only 32% Ni, it has high resistance to SCC and irradiation damage. Metal loss data of Alloy 800 have been measured up to 750 ºC and are presented in Figure 2. Note that cold-worked (ground) specimens tested by Leistikow [30] exhibited much lower metal loss than comparative tests with annealed specimens.

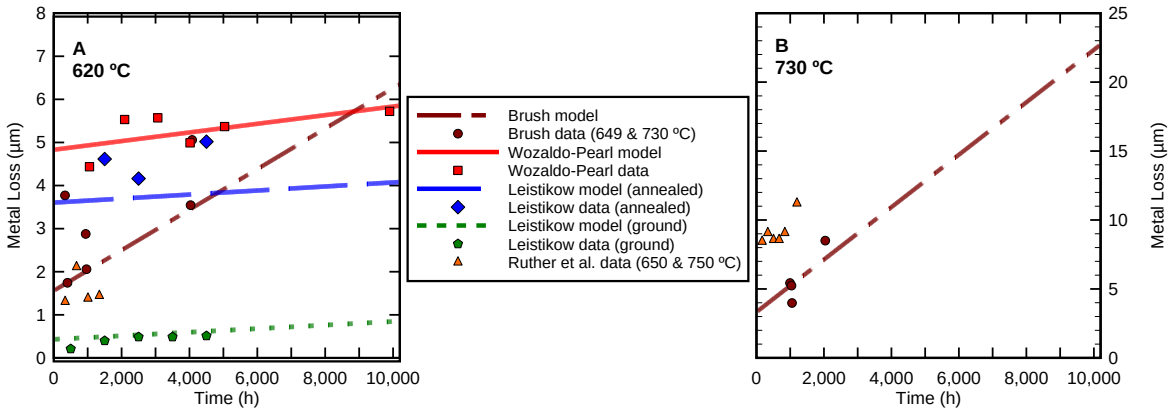

Figure 2: Data for Alloy 800 metal loss in superheated steam (symbols) and models (lines) applied at (A) 620 ºC and (B) 730 ºC for the length of one fuel cycle, 10 200 h. Data from Brush [31], Wazaldo and Pearl [32], Leistikow [30], and Ruther et al. [33].

Brush [31] presented an Arrhenius-like model for extending the descaled weight loss data obtained from heat transfer specimens to higher temperatures (Eqn. 8).

$$\Delta W = \Delta W_0 + k_l \cdot t$$
$$= 0.6102 \frac{\mu m}{K} \cdot T \cdot \exp\left(\frac{-5230}{T}\right) + 0.05966 \frac{\mu m}{d \cdot K} \cdot t \cdot T \cdot \exp\left(\frac{-10388}{T}\right) \quad (8)$$

At 830 ºC, the predicted corrosion metal loss of annealed Alloy 800 after 3 fuel cycles (30 600 h) is 170 µm. This is marginally less than the metal loss acceptance criteria of 200 µm, and does not consider fretting.

The inner oxide layer formed on Alloy 800 is usually found to be a mixture of Ni, Mn and Cr oxides, with outer layers consisting of Fe_3O_4 and α-Fe_2O_3 [25][30]. (Shot-peening results in more Cr-rich oxides and eliminates Fe_3O_4 [25].) The thermal expansion coefficients of these oxides differ from that of the metal, and the resulting stress is expected to cause oxide exfoliation [25] at a critical thickness of 15 µm [23]. From Eqn. 8, the expected metal contribution to oxide growth between fuel cycles is at most 57 µm or 4520 mg/dm^2, if there is no chromia evaporation. These oxides contain approximately 72 wt% metal and have densities around 5 g/cm^3, which suggests that the oxide growth between fuel cycles would be around 250 µm (at 50% porosity).

It has already been mentioned that cold-work like shot peening can reduce corrosion of Alloy 800, although there is some evidence that this effect disappears at high temperatures [23]. Aluminum addition to Alloy 800 has also been shown to reduce its overall corrosion [33].

Corrosion Penetration	170 µm at 830 ºC (30 600 h)
Inner Oxide / Outer Oxide	$Cr_2O_3/Fe_3O_4/Fe_2O_3$
Native Oxide Thickness	~250 µm (10 200 h)
Cracking Resistance	Good (32% Ni)

Table 2: Alloy 800 Scorecard

4. Alloy 625

Alloy 625 is a high-nickel alloy (58 wt%) with superior corrosion resistance and good fabricability. Its nickel content borders on the high end of the acceptable range for cracking resistance established by Coriou et al. [9]. Was et al. [34] exposed Alloy 625 to deaerated SCW at 500 ºC during a CERT test and noted a high crack density on the gage section. Wozaldo and Pearl [32] reported precipitation of M_6C at the grain boundaries of Alloy 625 exposed to 621 ºC steam that grew heavier with time (5691 h test). Its use as fuel cladding should therefore be approached with some caution.

Nonetheless, provided SCC can be dispositioned for the service conditions, the corrosion resistance of Alloy 625 is excellent. The corrosion of Alloy 625 has been measured up to 750 ºC in steam by several researchers (Figure 3).

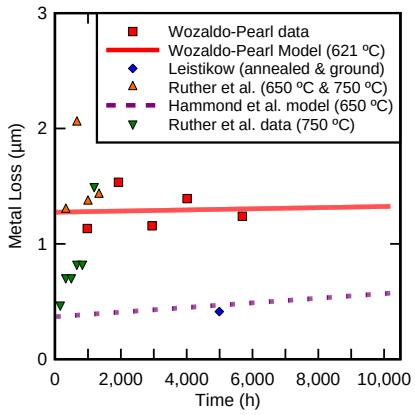

Figure 3: Alloy 625 metal loss data (symbols) and models (lines) applied for the length of one fuel cycle, 10 200 h. Data from Wazaldo and Pearl [32], Leistikow [30], Ruther et al. [33], and Hammond et al. [35].

Deodeshmukh [29] reported a constant rate of weight loss (presumably by evaporation of chromia) of 22 $mg \cdot dm^{-2} \cdot mo^{-1}$ for Alloy 625 in 871 ºC air with 10% steam. The total metal loss after 360 days under these conditions was 8 µm, with up to 28 µm oxide penetration into the matrix. While these results are not able to be directly translated to corrosion in SCW, they are encouraging. Assuming

the rate of oxygen diffusion is not significantly different in SCW, the total oxide penetration after 3 fuel cycles might be expected to be on the order of 100-150 µm.

The oxide layers formed on Alloy 625 are usually found to be primarily Cr_2O_3 with an outer layer of NiO [29][32]. Wazaldo and Pearl [32] noted some separation of the inner and outer layers, but did not expect significant exfoliation with time. They noted that the oxide thickness did not grow significantly with time [32]. The oxide thickness reported by Deodeshmukh in 760 ºC air with 10% steam was 3.5 µm [29] after 360 days. It is reasonable to expect that the oxide thickness at 830 ºC would be less than the acceptance criteria of 10 µm.

Corrosion Penetration	<2 µm at 650 and 750 ºC in steam up to 6000 h 28 µm at 871 ºC in air/10% steam (8640 h)
Inner Oxide / Outer Oxide	Cr_2O_3/NiO
Native Oxide Thickness	3.5 µm at 760 ºC in air/10% steam (8640 h)
Cracking Resistance	Caution (58% Ni)

Table 3: Alloy 625 Scorecard

5. Summary and Conclusions

Fuel cladding acceptance criteria were developed for metal loss and oxide thickness, and Alloys 214, 800 and 625 were evaluated with respect to these criteria. The most corrosion resistant of these was Alloy 214, which forms an alumina scale. None of the alloys are expected to retain an oxide thicker than 15 µm, which is important for maintaining a low temperature difference across the oxide, and all of the alloys have expected metal losses less than the acceptance criteria. However, without modification or surface treatment, Alloy 800 is expected to suffer severe oxide exfoliation, which will increase activity transport and erode turbine blades. Nonetheless, the lower Ni content of Alloy 800 is believed to lend it better resistance to SCC and irradiation damage.

Cold-work has been known to improve corrosion resistance at temperatures less than 650 ºC, but this benefit may not extend to higher temperatures. While cold-work improves the retained ductility of irradiated alloys, it reduces their initial ductility; and, some initial ductility is needed to collapse the cladding around the fuel. Further, cold-work is known to increase SCC susceptibility and increase the crack growth rate.

Future testing of candidate alloys is required to confirm the expected corrosion and SCC properties at temperatures up to 830 ºC in oxidizing SCW. Alloy 214 is not considered a prime candidate because of its high Ni content and cracking tendencies. A related alloy, HR-224, with 47.5% Ni may have better SCC resistance. Alloy 800 is expected to experience high corrosion rates that could compromise the cladding, and additional work is required to assess this and, if required, find ways to reduce the corrosion rate, such as through the addition of up to 4% Al. Alloy 625 shows superior corrosion resistance, although the internal penetration of oxides is not trivial and needs assessment. The SCC behaviour of Alloy 625 must be carefully investigated under representative conditions.

6. References

[1] B. Cox, "Accelerated Oxidation of Zircaloy-2 in Supercritical Steam", AECL-4448, 1973.

[2] A.T. Motta, A. Yilmazbayhan, M.J. Gomes da Silva, R.J. Comstock, G.S. Was, J.T. Busby, E. Gartner, Q. Peng, Y.H. Jeong and J.Y. Park, "Zirconium Alloys for Supercritical Water Reactor Applications: Challenges and Possibilities", Journal of Nuclear Materials, Vol. 371, Nos. 1-3, 2007, pp. 61-75.

[3] D. Khatamian, "Corrosion and Deuterium uptake of Zr-based Alloys in Supercritical Water", Journal of Supercritical Fluids, Vol. 78, 2013, pp. 132-142.

[4] R. Peraldi and B.A. Pint, "Effect of Cr and Ni Contents on the Oxidation Behavior of Ferritic and Austentitic Model Alloys in Air with Water Vapor", Oxidation of Metals, Vol. 61, Nos. 5/6, 2004, pp. 463-483.

[5] X. Ru and R.W. Staehle, "Historical Experience Providing Bases for Predicting Corrosion and Stress Corrosion in Emerging Supercritical Water Nuclear Technology: Part 1–Review", Corrosion, Vol. 69, No. 3, 2013, pp. 211-229.

[6] J. Bichoff, "Oxidation Behavior of Ferritic-Martensitic and ODS Steels in Supercritical Water", PhD Dissertation, Pennsylvania State University, 2011.

[7] J. Kaneda, S. Kasahara, J. Kuniya, K. Moriya, F. Kano, N. Saito, A. Shioiri, T. Shibayama and H. Takahashi, "General Corrosion Properties of Titanium Based Alloys for the Fuel Claddings in the Supercritical Water-cooled Reactor", Proceedings of the 12th International Conference on Environmental Degradation of Materials in Nuclear Power Systems-Water Reactors, Salt Lake City, Utah, USA, 2005 August 14-18.

[8] X. Ru and R.W. Staehle, "Historical Experience Providing Bases for Predicting Corrosion and Stress Corrosion in Emerging Supercritical Water Nuclear Technology–Part 2: Review", Corrosion, Vol. 69, No. 4, 2013, pp. 319-334.

[9] H. Coriou, L. Grall, P. Olivier and H. Willermoz, "Influence of Carbon and Nickel Content on Stress Corrosion Cracking of Austenitic Stainless Alloys in Pure and Chlorinated Water at 350 ºC", Proceedings of the International Conference on Fundamental Aspects of Stress Corrosion Cracking, Houston, TX, USA, 1967 September 11-15.

[10] T. Yonezawa and K. Onimura, "Effect of Chemical Compositions and Microstructure on the Stress Corrosion Cracking Resistance of Nickel-based Alloys in High Temperature Water", Proceedings of the International Conference on Evaluation of Materials Performance in Severe Environments (EVALMAT'89), Kobe, Japan, 1989 November 20-23, Tokyo, Japan: Iron and Steel Inst. Of Japan, Vol.1, pp. 235-242.

[11] X. Ru and R.W. Staehle, "Historical Experience Providing Bases for Predicting Corrosion and Stress Corrosion in Emerging Supercritical Water Nuclear Technology: Part 3–Review", Corrosion, Vol. 69, No. 5, 2013, pp. 423-447.

[12] G.S. Was, P. Ampornat, G. Gupta, S. Teysseyre, E.A. West, T.R. Allen, K. Sridharan, L. Tan, Y. Chen, X. Ren, and C. Pister, "Corrosion and Stress Corrosion Cracking in Supercritical Water", Journal of Nuclear Materials, Vol. 371, Nos. 1-3, 2007, pp. 176-201.

[13] S. Teysseyre, Z. Jiao, E. West and G.S. Was, "Effect of Irradiation on Stress Corrosion Cracking in Supercritical Water", Journal of Nuclear Materials, Vol. 371, Nos. 1-3, 2007, pp. 107-117.

[14] R. Xu, M. Yetisir and H. Hamilton, "Thermal-mechanical Behaviour of Fuel Element in SCWR Design", Proceedings of the 2014 Canada-China Conference on Advanced Reactor Development (CCCARD-2014), Niagara Falls, Ontario, Canada, 2014 April 27-30.

[15] F.A. Comprelli and U.E. Wolff, "Stability of High Nickel Alloys in Superheated Steam", General Electric, GEAP-4745, 1964.

[16] C. Sun, R. Hui, W. Qu and S. Yick, "Progress in Corrosion Resistant Materials for Supercritical Water Reactors", Corrosion Science, Vol. 51, No. 11, 2009, pp. 2508-2523.

[17] M.L. Grossbeck, K. Ehrlich and C. Wassilew, "An Assessment of Tensile, Irradiation Creep, Creep Rupture, and Fatigue Behavior in Austenitic Stainless Steels with Emphasis on Spectral Effects", Journal of Nuclear Materials, Vol. 174, Nos. 2-3, 1990, pp. 264-281.

[18] G.E. Lucas, "The Evolution of Mechanical Property Change in Irradiated Austentic Stainless Steels", Journal of Nuclear Materials, Vol. 206, Nos. 2-3, 1993, pp. 287-305.

[19] J. Pencer, D. Watts, A. Colton, X. Wang, L. Blomeley, V. Anghel and S. Yue, "Core Neutronics for the Canadian SCWR Conceptual Design", Proceedings of the 6th International Symposium on Supercritical Water-Cooled Reactors (ISSCWR-6), Shenzhen, Guangdong, China, 2013 March 03-07, Paper ISSCWR6-13021.

[20] N. Cinosi, I. Haq, M. Bluck and S.P. Walker, "The Effective Thermal Conductivity of Crud and Heat Transfer from Crud-coated PWR Fuel", Nuclear Engineering and Design, Vol. 241, 2011, pp. 792-798.

[21] D. Guzonas, F. Brosseau, P. Tremaine, J. Meesungnoen, and J.-P. Jay-Gerin, "Water Chemistry in a Supercritical Water-cooled Pressure Tube Reactor", Nuclear Technology, Vol. 179, No. 2, 2012, pp. 205-219.

[22] W.G. Cook and R.P. Olive, "Corrosion Product Deposition on Two Possible Fuel Geometries in the Canadian-SCWR Concept", Proceedings of the 3rd China-Canada Joint Workshop on Supercritical-Water-Cooled Reactors (CCSC-2012), Xi'an, China, 2012 April 18-20, Paper P83.

[23] J.M. Sarver and J.M. Tanzosh, "Effect of Temperature, Alloy Composition and Surface Treatment on the Steamside Oxidation / Oxide Exfoliation Behavior of Candidate A-USC Boiler Materials", Babcock & Wilcox Technical Paper BR-1898. Presented at Seventh International Conference on Advances in Materials Technology for Fossil Power Plants, Waikoloa, Hawaii, USA, 2013 October 22-25.

[24] L. Tan, T.R. Allen and Y. Yang, "Corrosion Behavior of Alloy 800H (Fe-21Cr-32Ni) in Supercritical Water", Corrosion Science, Vol. 53, No. 2, 2011, pp. 703-711.

[25] L. Tan, X. Ren, K. Sridharan and T.R. Allen, "Effect of Shot-peening on the Oxidation of Alloy 800H Exposed to Supercritical Water and Cyclic Oxidation", Corrosion Science, Vol. 50, No. 7, 2008, pp. 2040-2046.

[26] V.P. Deodeshmukh, S.J. Matthews and D.L. Klarstrom, "High-temperature Oxidation Performance of a New Alumina-forming Ni-Fe-Cr-Al Alloy in Flowing Air", International Journal of Hydrogen Energy, Vol. 36, No. 7, 2011, pp. 4580-4587.

[27] P. Kritzer, "Corrosion in High-temperature and Supercritical Water and Aqueous Solutions: A Review", Journal of Supercritical Fluids, Vol. 29, Nos. 1-2, 2004, pp. 1-29.

[28] A.S. Bakai, D.A. Guzonas, V.N. Boriskin, A.N. Dovbnya and S.V. Dyuldya, "Supercritical Water Convection Loop for SCWR Materials Corrosion Tests under Electron Irradiation: First Results and Lessons Learned", Proceedings of the 6th International Symposium on Supercritical Water-Cooled Reactors (ISSCWR-6), Shenzhen, Guangdong, China, 2013 March 03-07, Paper ISSCWR6-13062.

[29] V.P. Deodeshmukh, "Long-term Performance of High-temperature Foil Alloys in Water Vapor Containing Environment. Part I: Oxidation behavior", Oxidation of Metals, Vol. 79, Nos. 5-6, 2013, pp. 567-578.

[30] S. Leistikow, "Isothermal Steam Corrosion of Commercial Grade Austenitic Stainless Steels and Nickel Base Alloys in Two Technical Surface Conditions", Proceedings of the Fourth International Congress on Metallic Corrosion, Amsterdam, Netherlands, 1969 September 7-14. Houston, TX: National Association of Corrosion Engineers, 1972, pp. 278-290.

[31] E.G. Brush, "Corrosion-rate-law Considerations in Superheated Steam", Nuclear Applications, Vol. 1, No. 3, 1965, pp. 246-251.

[32] G.P. Wozaldo and W.L. Pearl, "General Corrosion of Stainless Steels and Nickel Base Alloys Exposed Isothermally in Superheated Steam", Corrosion, Vol. 21, No. 11, 1965, pp. 355-369.

[33] W.E. Ruther, R.R. Schlueter, R.H. Lee and R.K. Hart, "Corrosion Behavior of Steels and Nickel Alloys in Superheated Steam", Corrosion, Vol. 22, No. 5, 1966, pp. 147-155. Presented at 21st Conference, National Association of Corrosion Engineers, St. Louis, Missouri, USA, 1965 March 15-19.

[34] G.S. Was, S. Teysseyre and J. McKinley, "Corrosion and Stress Corrosion Cracking of Iron - and Nickel-base Austenitic Alloys in Supercritical Water", Proceedings of Corrosion NACExpo 2004, New Orleans, LA, 2004 March 28-April 1. Houston, TX: NACE, 2004, Paper No. 04492.

[35] J.P. Hammond, P. Patriarca, G.M. Slaughter and W.A. Maxwell, "Corrosion of Incoloy 800 and Nickel Base Alloy Weldments in Steam", Welding Journal, Vol. 52, No. 6, 1973, pp. 268s-280s, Welding Research Supplement.